Title: Omega–3 encapsulation by PGSS-drying and conventional drying methods. Particle characterization and oxidative stability

Authors

Rodrigo Melgosa (rmgomez@ubu.es)

Óscar Benito (obenito@ubu.es)

María Teresa Sanz* (tersanz@ubu.es)

Esther de Paz (ede@ubu.es)

Sagrario Beltrán (beltran@ubu.es)

Address

Department of Biotechnology and Food Science (Chemical Engineering Section)

University of Burgos, Plaza Misael Bañuelos s/n 09001 Burgos, Spain

* Corresponding author. Tel.: +34-947258810; Fax: +34-947258831; e-mail: tersanz@ubu.es

Abstract

Particles from Gas-Saturated Solutions (PGSS)-drying has been used as a green alternative to encapsulate omega–3 polyunsaturated fatty acids (*n*–3 PUFAs) at mild, non-oxidative conditions. PGSS-dried particles have been compared to those obtained by conventional drying methods such as spray-drying and freeze-drying, finding encapsulation efficiencies (EE) up to 98 % and spherical morphology for PGSS- and spray-dried particles. Freeze-dried powders showed irregular morphology and EE from 95.8 to 98.6 %, depending on the freezing method. Differential scanning calorimetry (DSC) analysis revealed glass-transition and melting peaks of OSA-starch and a cold-crystallization peak corresponding to the encapsulated *n*–3 PUFA concentrate. Compared to conventionally dried powders, PGSS-dried microparticles showed lower primary and secondary oxidation after 28 days of storage at 4 ºC. Ascorbic acid addition combined with the mild processing conditions of PGSS-drying yielded particles with a maximum peroxide value of 2.5 meq O_2/kg oil after 28 days of storage at 4 ºC.

1. Introduction

An adequate intake of omega–3 polyunsaturated fatty acids (*n*–3 PUFAs) is recommended in healthy diet guidelines due to their important benefits (Ruxton, Reed, Simpson, & Millington, 2004). Long-chain *n*–3 PUFAs, mainly eicosapentaenoic (EPA, 20:5 *n*–3) and docosahexaenoic (DHA, 22:6 *n*–3) acids are eicosanoid precursors, which are immunomodulatory molecules with a key role in the inflammatory response. EPA and DHA are claimed to contribute to the normal brain, eye and cardiovascular functions in adults and help in the normal development of the eyes, the brain and the nervous system in children (EFSA, 2010).

The perceived health benefits of these compounds have created a strong demand for EPA and DHA concentrates in the pharmaceutical and food industries. However, *n*–3 PUFAs are unstable and very prone to oxidation, easily generating lipid hydroperoxides and free radicals under oxidative conditions. These species negatively affect sensory properties, since they can decompose into low-molecular-weight volatile compounds that are perceived as rancid, and what is more, they present potentially cytotoxic, carcinogenic and mutagenic effects (Niki, 2009; Uluata, McClements, & Decker, 2015) For these reasons, *n*–3 PUFA concentrates are often encapsulated in order to protect them from light and oxygen during shelf life; and natural antioxidants such as tocopherols, phospholipids, ascorbic acid, or their mixtures are usually added (Baik et al., 2004; Löliger & Saucy, 1994).

Materials of different nature can be used as *n*–3 PUFA encapsulating agents: proteins such as whey protein isolate, sodium caseinate or gelatin, phospholipids such as lecithin, or polysaccharides such as gum Arabic, carboxymethyl cellulose, maltodextrin, chitosan, or modified starch are some examples of carrier materials for microencapsulation of oils rich in *n*–3 PUFAs (Encina, Vergara, Giménez, Oyarzún-

Ampuero, & Robert, 2016). Among them, *n*-octenyl-succinic-anhydride modified starch (OSA-starch) has been chosen in this work because it presents good emulsifying properties and is suitable to encapsulate oils rich in *n*–3 PUFAs, as well as other bioactive compounds such as essential oils and hydrophobic compounds (Carneiro, Tonon, Grosso, & Hubinger, 2013; de Paz, Martín, Bartolomé, Largo, & Cocero, 2014; Drusch, Serfert, Scampicchio, Schmidt-Hansberg, & Schwarz, 2007; Jafari, Assadpoor, He, & Bhandari, 2008; Varona, Martín, & Cocero, 2011).

Different encapsulation techniques can be used to encapsulate *n*–3 PUFAs, such as emulsification, spray-drying, freeze-drying, coacervation, *in situ* polymerization, extrusion, or fluidized-bed coating (Bakry et al., 2016). Among these, the most widely used technique in the food and pharmaceutical industries is spray-drying, followed by freeze-drying. Freeze-drying is often applied to thermolabile and easily oxidizable compounds due to the protective low temperatures and vacuum conditions involved in the process. Its main drawback is the energy consumption, linked to the low temperature and high vacuum conditions as well as the long residence times required to completely dry the product, which in turn translate into high processing costs. On the contrary, spray-drying is a low-cost microencapsulation technology which operates in a relatively simple and continuous way, thus it is commonly used at industrial scale (Bakry et al., 2016).

Prior to the drying step, the non-soluble *n*–3 PUFAs need to be dispersed into the encapsulating agent solution, obtaining an oil-in-water (O/W) emulsion. Several methods can be used to prepare O/W emulsions, such as conventional emulsification (colloid milling, high speed blending and high-pressure homogenization), ultrasound (US) assisted emulsification, membrane emulsification, and micro-channel emulsification (Chatterjee & Judeh, 2015). Among them, US-assisted emulsification has

grown in importance among the pharmaceutical, cosmetic, and food industries, thanks to its versatility and the possibility of obtaining high quality food products with enhanced functional properties (Abbas, Hayat, Karangwa, Bashari, & Zhang, 2013). US-assisted emulsification can be applied to improve stability and bioavailability of the dispersed bioactive compounds and, in particular, it can be used to obtain O/W emulsions with nanometric droplet size and narrow size distribution. Typically, US-assisted emulsification consists on applying low-frequency sound waves of 20-100 kHz through a metallic sonotrode immersed in the liquid medium, in order to generate disruptive forces that break down the macroscopic phases to nanosize droplets. The nano-scale emulsions obtained present interesting functional properties and enhanced stability against oxidation (Abbas et al., 2013).

Supercritical fluids, and particularly supercritical carbon dioxide (SC-CO_2), are a convenient medium to produce particles loaded with bioactive compounds. Carbon dioxide is an inert, non-toxic solvent, and is completely released from the product as a gas once back to atmospheric conditions. Besides, the accessibility of the supercritical state of carbon dioxide (T_C = 31.1 °C; p_C = 73.8 bar) and its advantageous physical properties (high density and diffusivity, and low viscosity) make SC-CO_2 the solvent of choice in many particle formation processes. (Türk, 2014). Among the several available techniques, the Particles from Gas Saturated Solutions (PGSS) process overcomes the problems of solubility limitations and high gas consumption of other particle formation methods using SC-CO_2 (Türk, 2014). This technique can be used for drying aqueous solutions, dispersions or, as in this work, O/W emulsions, in the so-called PGSS-drying process (Türk, 2014).

Basically, the PGSS-drying technique consists on mixing an aqueous solution with supercritical carbon dioxide upon saturation, and subsequently expanding the gas-

saturated solution down to atmospheric pressure through a nozzle. This technique can be used as an alternative to conventional spray-drying, achieving a more efficient atomization due to the sudden vaporization of the dissolved CO_2 and the expansion of gas bubbles in the solution during depressurization from supercritical to atmospheric conditions. Both effects improve the atomization of the sprayed solution forming small droplets, thus reducing the particle size of the dried powder and enhancing the drying process (Martín & Weidner, 2010; Weidner, 2009). Besides, and because of the intense and deep cooling caused by the Joule-Thomson effect, it is possible to dry the product at low temperature (40-80 ºC) (de Paz, Martín, & Cocero, 2012; Weidner, 2009). The mild-temperature conditions, combined with the intrinsically inert atmosphere due to oxygen displacement, prevent, or at least delay, oxidative degradation of the encapsulated bioactive compounds (de Paz et al., 2012; Weidner, 2009). Operating conditions in the spray tower, particularly temperature and gas-to-product ratio (GPR), must be taken into account in order to operate above the dew line of the carbon dioxide–water system (Martín & Weidner, 2010), and ensure the complete drying of particles.

In this work, an *n*–3 PUFA enriched fish oil has been encapsulated by the alternative and green technology Particles from Gas Saturated Solutions (PGSS)-drying. The main hypothesis of the study is to explore whether or not the potential benefits of supercritical carbon dioxide technologies applied to particle formulation and encapsulation may affect particle properties and oxidative stability of heat-sensitive and easily oxidizable compounds such as *n*–3 PUFAs, compared to other conventional drying methods. This way, the PGSS-dried particles have been compared to those obtained by spray-drying and freeze-drying, which are commonly applied in the pharmaceutical, cosmetic, and food industries to dry aqueous solutions and dispersions. Characterization of the particles obtained by the different drying methods has been

130 performed in terms of particle morphology, residual humidity, and particle size
131 distribution of the reconstituted particles. Besides, encapsulation efficiency and
132 oxidative stability (primary and secondary oxidation) of the encapsulated n–3 PUFA
133 concentrate have been monitored over time in the particles formulated with each of the
134 drying methods. Additionally, an antioxidant (ascorbic acid) has been added to some of
135 the formulations as a strategy to potentially enhance the oxidative stability of the
136 encapsulated *n*–3 PUFA concentrate.

137

138 2. Materials and methods

139 2.1. Materials

140 *n*–3 PUFA concentrate from fish oil, Algatrium™ Plus, was kindly donated by Brudy
141 Technology S.L. (Spain). It has been stored at 4 ºC in darkness and N_2 atmosphere. Hi-
142 Cap™ 100, an octenyl-succinic-anhydride modified starch (OSA-starch) derived from
143 waxy maize, was provided by Ingredion Inc. (Germany). Carbon dioxide (99.9%) was
144 provided by Air Liquide S.A. (Spain). Ascorbic acid (L(+)-Ascorbic acid, AA) was
145 purchased from Panreac AppliChem (Spain).

146 37% hydrochloric acid (HCl), diethyl ether, 1-butanol, 2-propanol, methanol, 2-
147 thiobarbituric acid (TBA), and trichloroacetic acid (TCA) were provided by VWR
148 Chemicals (Germany). Hexane, absolute ethanol, Iron(II) sulphate heptahydrate, and
149 ammonium thiocyanate were purchased from Merck KGaA (Germany). 2,2,4-
150 trimethylpentane (isooctane) and barium chloride dihydrate were supplied by Macron
151 Fine Chemicals (France) and Panreac AppliChem (Spain), respectively. Cumene
152 hydroperoxide and 1,1,3,3-tetraethoxypropane (TEP) standards were purchased from
153 Sigma Aldrich (USA).

2.2. Characterization of the *n*–3 PUFA concentrate

Neutral lipid profile of the *n*–3 PUFA concentrate has been analyzed by normal-phase HPLC (NP-HPLC). Separation was carried out at room temperature in a Lichrospher Diol column (5 mm, 4 mm×250 mm) and detection was performed by evaporative light scattering (ELSD) (Agilent Technologies 1200 Series, USA) at 35 ºC and 3.5 bar. Solvent gradient and calibration procedure have been reported elsewhere (Solaesa, Sanz, Falkeborg, Beltrán, & Guo, 2016).

Fatty acid profile of the *n*–3 PUFA concentrate has been determined according to the AOAC Official Method (*AOAC International*, 2012) in a Hewlett Packard gas chromatograph (6890N Network GC System) equipped with an auto-sampler (7683B series) and a flame ionization detector (FID). The separation was carried out in a fused silica capillary column (Omegawax-320, 30 m×0.32 mm i.d.) with helium (1.8 mL/min) as carrier gas. Injection and detection temperatures, as well as ramp conditions have been previously reported (Rebolleda, Rubio, Beltrán, Sanz, & González-San José, 2012). Most of the fatty acids were identified by comparison of their retention times with those of chromatographic standards (Sigma Aldrich). As indicated by the AOAC Official Method (*AOAC International*, 2012), an internal standard (methyl-tricosanoate, C23:0) was used for quantification purposes.

HPLC with diode array detection (HPLC-DAD) of the *n*–3 PUFA concentrate was carried out in order to detect tocopherol isomeric forms and other vitamin E analogs added to the *n*–3 PUFA concentrate, as their presence was reported by the provider. The analytical method is based on the IUPAC official method (Pocklington & Dieffenbacher, 1988) with slight modifications, as reported in Rebolleda et al., (2012).

Separation was performed in an ACE 5 silica 250 mm × 4.6 mm column with 1 mL/min of hexane:2- propanol (99:1) as the mobile phase. An isocratic gradient was used, and the total run time was 15 min. α-, β-, γ-, and δ-tocopherols were monitored at λ = 296 nm. For identification and quantification of each tocopherol isomer, a calibration curve with different amounts of the respective standard compound (Sigma Aldrich) was constructed.

2.3. Ultrasound-assisted emulsification

O/W emulsions were formulated in a weigh proportion of 70:24:6 (water:carrier:*n*–3 PUFA concentrate), which in preliminary experiments was found to be the optimal in terms of obtaining the smallest droplet size. First, an aqueous solution of the encapsulating agent was prepared by dissolving 24.0 g of Hi-Cap™ 100 in 70.0 mL of distilled water. Subsequently, 6.0 g of *n*–3 PUFA concentrate were added drop by drop to the carrier solution under continuous stirring. Then, the mixture was stirred for 5 minutes to obtain a pre-emulsion, which was subsequently processed in a 20 kHz 750 W ultrasonic liquid processor Vibra-Cell 75043 (Sonics & Materials Inc.) with a Ø13 mm titanium alloy sonotrode. Based on previous studies, amplitude was set at 100 % and sound waves were delivered in pulses (5 s On/5 s Off) in order to avoid excessive heating of the sample, for a total processing time of 180 s. O/W emulsions were produced in batches of 100 g.

2.4. PGSS-drying

O/W emulsions were processed using the PGSS-drying technique in order to remove water and obtain a solid powder with the encapsulated *n*–3 PUFA concentrate loaded

202 into the OSA-starch microparticles. Fig. 1 presents the schematic flow diagram of the
203 PGSS-drying apparatus, in which CO_2 was fed by a membrane pump (LEWA) and
204 preheated using a silicone bath before injection into the static mixer, where it was mixed
205 with the O/W emulsion at the selected pressure and temperature. The CO_2 mass flow
206 rate was measured with a Coriolis flow meter (Danfoss) with an accuracy of ± 0.1 kg
207 CO_2/h. Temperature before and after the static mixer was measured by means of Pt100
208 thermoresistances (accuracy of ± 0.1 K), being the later under PID control. Pressure in
209 the CO_2 line and after the static mixer was measured with pressure transmitters (DESIN
210 Instruments) with an accuracy of ± 0.05 MPa. Bourdon manometers (Nuova Firma)
211 were installed to provide secondary lectures of the operating pressure.

212 The O/W emulsion was pumped into the static mixer by a GILSON 305 piston pump
213 (max. flow rate: 25 ± 0.1 mL/min). The gas-saturated emulsion was then expanded into
214 the spraying tower through a capillary nozzle with an internal diameter of 400 µm
215 (Spraying Systems Co., Ref.: PF1650-SS). The spraying tower was made of PVC and
216 heated by electrical resistances. Temperature in the spray tower was also measured with
217 a Pt100 probe and controlled using a PID. CO_2 was vented off the spraying tower and
218 passed through a water vapor condenser before final release. As security elements, a
219 rupture disk, check valves, and a relief valve were installed at different points in the
220 high-pressure circuit.

221 Typically, a PGSS-drying experiment began with the preheating of the system up to the
222 desired temperature in the static mixer, fixed at 110 ºC, and in the spraying tower,
223 which was set at 55 ºC. When temperature was achieved, CO_2 was pumped up to the
224 desired pressure, which was fixed at 10.0 MPa. Pressure in the static mixer and
225 temperatures in the static mixer and the spraying tower were selected based on previous
226 studies (Varona et al., 2011). Once temperature and pressure conditions were stable, the

emulsion pump was started at a flow rate such that the desired GPR, which was selected at 30 g/g, was obtained. After all the O/W emulsion was processed, CO_2 was allowed to flow through the system at the same pressure and temperature conditions during 15 minutes in order to completely dry the particles. After that, the system was depressurized and particles were collected from the walls and bottom of the spraying tower and stored in darkness and refrigeration at 4 ºC for subsequent analyses.

2.5. Spray-drying

Spray-drying is a conventional, well-known drying technique which is widely used in the pharmaceutical, cosmetic and food industries; thus, it was chosen to compare the characteristics of the powder that may be obtained conventionally to those of the powder obtained by the alternative PGSS-drying process. The spray-drying process was carried out in a commercial Buchi B-290 mini Spray-dryer. The O/W emulsion, obtained as described in section 2.3, was fed into the spray-drying apparatus at an inlet temperature of 155 ºC, and %pump of 8 %, which was equivalent to a mass flow of emulsion of 3.0 g/min. Outlet temperature was 100 ºC. The emulsion was sprayed through a nozzle with 1.5 mm diameter and dried under a N_2 flow of 360 L/h.

2.6. Freeze-drying

O/W emulsions obtained by the US-assisted method described in section 2.3 were submitted to two different freezing methods: (1) conventional at -20 ºC overnight, and (2) freezing with liquid nitrogen (-196 ºC). Samples were then equilibrated at -80 ºC for 2 h and submitted to freeze-drying in a Labconco Freeze Dry System at $1.5 \cdot 10^{-4}$ mbar during 48 h. These two different freezing methods were chosen in order to evaluate the

effect of the freezing step, since the slower conventional freezing process is more likely to form large crystals of water, which could adversely affect the emulsion stability and structure, whereas the rapid freezing achieved with liquid nitrogen could better preserve the physical structure of the emulsion.

2.7. Characterization of the O/W emulsion

2.7.1. Droplet size analysis of the O/W emulsions

The droplet size distribution of the O/W emulsions (original and reconstituted) was measured by a Laser Diffraction (LD) equipment (Malvern Mastersizer 2000). A small amount of sample was suspended in the suspension container filled with distilled water under gentle agitation. In the case of the reconstituted O/W emulsions, the dried powders were firstly dissolved in distilled water, maintaining the original ratio of 70:24:6 wt. (water:carrier:*n*–3 PUFA concentrate).

Droplet size measurements are reported as relative volume distribution and defined by the mean diameter over volume (DeBroukere mean, D[4,3]) and the volume/surface mean diameter (Sauter mean, D[3,2]), calculated as in Eqs. 1 and 2, respectively.

$$D[4,3] = \frac{\sum_{1}^{n} D_{i}^{4} v_i}{\sum_{1}^{n} D_{i}^{3} v_i} \quad (1)$$

$$D[3,2] = \frac{\sum_{1}^{n} D_{i}^{3} v_i}{\sum_{1}^{n} D_{i}^{2} v_i} \quad (2)$$

where D_i is the diameter of the *i*th particle.

The median particle size ($d_{0.5}$), defined as the maximum particle diameter below which 50 % of the sample volume exists, is also reported. The span value, defined in Eq. 3, was also calculated.

$$\text{span} = \frac{d_{0.9} - d_{0.1}}{d_{0.5}} \quad (3)$$

where d_x is the maximum particle diameter below which x% of the sample volume exists. Span values near to 1 indicate a narrow particle size distribution (PSD).

2.7.2. Emulsion stability

Physical stability of the O/W emulsion was analyzed by static multiple scattering in a vertical scan analyzer Turbiscan Lab Expert (Formulaction Inc.) with ageing station AGS. By means of two optical sensors, the instrument measures the light transmitted through the emulsion (180º from the incident light, transmission, T) and the light backscattered by the emulsion droplets (45º from the incident light, backscattering, BS). The scanning process is made vertically along the glass cell from bottom to top, and the T/BS are each plotted as a function of the emulsion height in the glass cell. By monitoring the T/BS profiles at different time intervals, physical changes in the emulsion can be followed over time, which gives a detailed overview of dispersion stability or instability. In the current work, the stability of the original emulsion was monitored at 4 h intervals during 24 days. Emulsion samples were kept in the ageing station at a constant temperature of 25 ºC. As variations in T profiles were lower than 2%, only BS profiles at different storage times were analyzed in this study.

2.7.3. Density of the O/W emulsions

Density of the O/W emulsions was measured in an Anton Paar DMA 5000 instrument at 25 ºC. Measurements were carried out in triplicate.

2.8. Characterization of the dried powders

2.8.1. Yield, moisture, encapsulation efficiency and bioactive loading

Yield of particles was calculated as the ratio between the mass of collected particles ($m_{collected\ particles}$) and the theoretical mass fed to the PGSS-drying, spray-drying, or freeze-drying apparatus $m_{initial\ feed}$, expressed as weight percentage (Eq. 4).

$$\text{Yield}\ (\%) = \frac{m_{collected\ particles}}{m_{initial\ feed}} \cdot 100 \quad (4)$$

Moisture content of the dried particles was determined gravimetrically. Samples (*ca*. 0.5 g) of particles obtained by the different methods used in this work were weighed before and after drying in an oven at 120 ºC until constant weight.

Encapsulation efficiency (EE) was determined according to the method described by Wang *et al.* (Y. Wang, Liu, Dong, & Selomulya, 2016) with some modifications. For the non-encapsulated oil determination, samples (*ca*. 1.0 g) of particles obtained by the different methods used in this work were suspended with 25 mL of hexane in a Falcon centrifuge tube, which was vortexed for 15 s at room temperature and centrifuged at 3000 rpm during 20 min. Immediately afterwards, the supernatant was taken and filtered, and its oil content was measured spectrophotometrically at λ = 286 nm. The same procedure was repeated two additional times to extract the potentially remaining non-encapsulated oil. A calibration curve was previously constructed with known quantities of *n*–3 PUFA concentrate dissolved in hexane.

315 Total oil in the dried particles obtained by the different methods used in this work was
316 determined by acid digestion of approximately 1.0 g of powder with 37% HCl, and
317 subsequent extraction with diethyl ether and petroleum ether, following the AOAC
318 Official Method (*AOAC International*, 2005). After centrifugation at 3000 rpm during
319 20 min, the solvent phase with the extracted oil was taken and transferred to tared
320 round-bottom flasks in order to evaporate the solvent under vacuum (Heidolph rotary
321 evaporator). Total oil in the samples was determined by mass difference of the initial
322 clean round-bottom flask and that containing the extracted oil residue. As a blank, the
323 same procedure was also followed with known quantities (*ca.* 1.0 g) of the carrier alone
324 (Hi-Cap™ 100). The fat traces found in the carrier were subtracted from the total oil
325 content of the powders.

326 Encapsulation efficiency (EE) was calculated from Eq. 5.

327 $$\mathrm{EE}\ (\%) = \frac{\mathrm{TO} - \mathrm{nEO}}{\mathrm{TO}} \cdot 100 \qquad (5)$$

328 where TO is the total oil content and nEO is the non-encapsulated oil.

329 The bioactive loading, which is also an important parameter of microencapsulated
330 bioactive compounds (Encina et al., 2016), has been also calculated. It can be referred
331 as to the total oil content (TO), expressed as mg oil/g sample.

332

333 ***2.8.2. Particle size analysis of the dried powders***

334 Particle size analysis of the dried powders was carried out in a Malvern Mastersizer
335 2000 equipment, following the same procedure as in the original O/W emulsion (see
336 section 2.7.1), yet dispersing the particles in absolute ethanol to avoid dissolution of the
337 encapsulating agent.

2.8.3. Scanning electron microscopy (SEM)

Morphology of the dried particles was observed in a Scanning Electron Detector microscope JEOL JSM-6460LV with Energy Dispersive X-ray (JEOL Ltd. Japan) operating at 20 kV. Samples were gold-sputtered and observed with magnifications of 1500, 5000 and 10000x for PGSS- and spray-dried particles, and 50, 400 and 2000 or 3000x for the freeze-dried powders.

2.8.4. Differential scanning calorimetry (DSC)

A TA Instruments Q200 differential scanning calorimeter with refrigerated cooling system (RCS90) and nitrogen purge gas was used. Melting point and enthalpies of indium were used for temperature and heat capacity calibration. Samples (*ca.* 10 mg) were placed in TA Tzero 40-μL aluminum pans and closed with hermetic aluminum lids with a pinhole. An empty pan closed with pinholed lid was used as a reference. Starting temperature of the DSC analysis was set at 40 ºC, and held for 30 min. Then, the system was cooled down to -80ºC at 10ºC·min^{-1}. After an isothermal period of 30 min, samples were heated from -80 ºC to 350 ºC at a constant heating rate of 10ºC·min^{-1}. DSC thermograms were recorded and analyzed with the Advantage v. 5.5.20 software (TA Instruments).

2.9. Measurement of lipid oxidation

Oxidative status of the dried powders was determined in terms of primary oxidation (peroxide value, PV) and secondary oxidation (Thiobarbituric Acid Reactive Substances, TBARS). To observe the effect of each drying method, PV and TBARS

were determined in the *n*–3 PUFA concentrate, as well as in the O/W emulsions before drying.

For the dried powders, PV and TBARS were measured right after each drying method (PGSS-drying, spray-drying, and freeze-drying) and monitored over a 28-day storage period. Dried powders were placed in closed containers and stored at 4 ºC in darkness. Samples were withdrawn at 7-day intervals and dissolved in distilled water to obtain reconstituted emulsions with the original water:carrier:*n*–3 PUFA concentrate proportion (70:24:6 wt.). PV and TBARS analyses were carried out as described below.

2.9.1. Peroxide Value

PV was measured spectrophotometrically with a Hitachi U-2000 apparatus and following the method described by Shanta *et al.* (Shantha & Decker, 1994) with slight modifications. In brief, 10-50 mg of oil or 0.025-1.0 mL of emulsion, depending on the expected PV, were taken in a centrifuge tube and mixed with 1.5 mL of isooctane:2-propanol (3:1 v/v). The tube was vortexed for 15 s and centrifuged at 5000 rpm during 10 min. Immediately afterwards, 0.2 mL of the supernatant were transferred to a new centrifuge tube and 2.8 mL of methanol:1-butanol (2:1 v/v) were added. After vortexing for 15 s, 15 μL of 3.94 M ammonium thiocyanate and 15 μL of a Fe^{2+} solution were added. The Fe^{2+} solution was obtained by mixing 0.132 M barium chloride in 0.4 M HCl and 0.144 M Iron(II) sulphate heptahydrate (1:1 v/v), centrifuging at 5000 rpm for 10 min, and taking the supernatant. Samples were vortexed again for 15 s and kept in darkness for 20 min. Blanks were prepared the same as above with 0.3 mL of distilled water instead of the oil or emulsion sample. Hydroperoxyde concentration was determined spectrophotometrically at λ = 510 nm. A calibration curve was constructed

using known concentrations of cumene hydroperoxide, ranging from 0.13 to 3.28 mM. Results were expressed in milliequivalents of oxygen per kg of *n*–3 PUFA concentrate (meq O_2/kg oil).

2.9.2. TBARS analysis

TBARS present in the *n*–3 PUFA concentrate were determined following the method described by Ke and Woyewoda (Ke & Woyewoda, 1979). Briefly, 10 mg of *n*–3 PUFA concentrate were weighed in a screw-capped glass test tube. 5 mL of TBA work solution, which was prepared by mixing 0.04 M 2-thiobarbituric acid in glacial acetic acid, chloroform, and 0.3M sodium sulphite (12:8:1 v/v), were also added to the screw-capped glass test tube. The mixture was vortexed for 15 s and incubated in a water bath at 95 ºC during 45 min. After cooling down the test tubes under running cold water, 2.5 mL of 0.28 M trichloroacetic acid were added to the samples, which were then mixed by inversion. Samples were then centrifuged at 2500 rpm for 10 min in order to separate the pink aqueous phase from the chloroform phase. Absorbance of the aqueous phase was measured at λ = 538 nm in a Hitachi U-2000 spectrophotometer. Blanks were prepared the same as above, yet without the oil, and subtracted from the absorbance measurement.

TBARS analysis of the original and reconstituted O/W emulsions was carried out following the method described by Mei *et al*. (Mei, McClements, Wu, & Decker, 1998) with slight modifications. Briefly, 0.025-1.0 mL of emulsion, depending on the expected oxidative status, were taken in screw-capped glass test tubes. Distilled water was used to complete to 1.0 mL if necessary. Subsequently, 2 mL of a TCA/TBA mixture – which was prepared by dissolving 7.5 g of TCA into 10 mL of 0.25M HCl,

adding this solution to 0.1875 g of TBA and completing to volume with 0.25M HCl in a 50 mL volumetric flask – were added and the glass test tube was tightly closed, vortexed for 15 s and immersed in a water bath at 95 ºC during 15 min. Then the vials were cooled down under running cold water and centrifuged at 5000 rpm during 10 min. Immediately afterwards, the supernatant was collected and its absorbance measured in a Hitachi U-2000 spectrophotometer at λ = 538 nm. Blank runs were also performed the same as above, but without adding the emulsion, and its absorbance subtracted from the measurements.

TBARS concentration in the emulsion and the *n*–3 PUFA concentrate samples was determined using a TEP standard curve with concentrations ranging from 2.5 to 20 nM. Results were expressed in mg malondialdehyde equivalents (MW = 72.06 g/mol) per kg of *n*–3 PUFA concentrate (mg MDA/kg oil).

2.10. Statistical analysis

All results reported in this work represent the average of at least three independent measurements. Drying experiments performed in this work have been duplicated. Statistical analyses were performed using Statgraphics Centurion XVII software. Statistical significance was determined by analysis of variance (ANOVA) using the Fisher's least significant difference test. Results were deemed as statistically significant when $p < 0.05$.

3. Results and discussion

3.1. Characterization of the *n*–3 PUFA concentrate

Results obtained in the characterization analysis are summarized in Table S-1 of the provided supplementary material. As it can be seen from Table S-1a, the fatty acid profile of the *n*–3 PUFA concentrate is constituted by more than 90 % *n*–3 PUFAs, being 73.49 % identified as DHA. Neutral lipid profile of the *n*–3 PUFA concentrate (Table S-1b) showed that more than the 75 % of the neutral lipids in the *n*–3 PUFA concentrate are in the form of triacylglycerides, with 21.6 % being in the form of fatty acid ethyl-esters. Traces of diacylglycerides and monoacylglycerides (1.2% and 0.7 %, respectively) were also found. The high content of triacylglycerides is an important feature of the *n*–3 PUFA concentrate, since these compounds are the natural form of food lipids and they may present better bioavailability and stability against oxidation (Rubio-Rodríguez et al., 2010). Tocopherol analysis by HPLC-DAD revealed a racemic mixture of tocopherol added as antioxidant (again, this is in consonance with consumer's preference for natural sources). α-, β-, γ-, and δ-tocopherol isomers were identified and quantified. Results are showed in Table S-1c.

3.2. Characterization of the O/W emulsion

3.2.1. Droplet size of the O/W emulsions

Results from the analysis of droplet size distribution are reported in Table 1 for the original and reconstituted O/W emulsions. In general, similar values for D[4,3] and D[3,2] were found in all samples, with the exception of the conventionally freeze-dried powder that showed significantly higher values for both D[4,3] and D[3,2], which

means that the reconstituted emulsion from the conventionally freeze-dried powder presented larger mean diameters both in volumetric and surface basis, respectively.

Median droplet size by volume ($d_{0.5}$) of the emulsion is sub-micrometric, with $d_{0.5}$ = 0.114 μm and a D[4,3] and D[3,2] of 0.144 μm and 0.114 μm, respectively. On the other hand, the drying methods proposed in this work significantly increased $d_{0.5}$ after reconstitution, with the exception being the freeze-dried particles with liquid N_2, in which no statistically significant differences were found with the original emulsion (p < 0.05). Still, most droplet populations were around 0.130 μm for particles obtained by PGSS-drying, freeze-drying and spray-drying methods, which demonstrates that the proposed drying methods do not produce aggregation of oil droplets. The span values followed the same trend as $d_{0.5}$, with original emulsion < freeze-drying (liq N_2) < spray-drying ≈ freeze-drying (-20 ºC) < PGSS-drying. The higher span values in the reconstituted emulsions may be due to higher polydispersity.

3.2.2. Emulsion stability

Physical stability of the US-assisted O/W emulsion was analyzed by static multiple scattering. Changes in the backscattering profile (ΔBS) of the O/W emulsion sample were recorded every 4 h during 24 days of storage at 25 ºC and plotted vs. time. Results are provided as supplementary material in Fig. S-1. As shown in this figure, ΔBS in the top-section reached 5% increment on day 2 and started to decrease in the lower section (|ΔBS| > 2%) on day 5, indicating creaming destabilization due to phase separation and migration of the lighter oil droplets to the top zone. Moreover, a slight BS increase over time in the middle section of the glass cell can be seen (Fig. S-1), indicating emulsion droplet size slightly increased over the 24-day storage period.

3.2.3. Density of the O/W emulsions

Density measurements were carried out for the original emulsion as well as for the reconstituted dried powders. Results obtained are shown in Table 1.

No statistical difference ($p < 0.05$) was found between the densities of the original and reconstituted emulsions, being those the means of three independent measurements. Thus, the average value of 1.091281 $g \cdot cm^{-3}$ was used for the volume-to-mass transformations necessary in the PV and TBARS calculations.

3.3. Characterization of the dried powders

3.3.1. Yield and bioactive loading

Calculated yield of particles and loading of fish oil concentrate of each of the proposed drying methods is showed in Table 1. The spray-drying method exhibits the lowest yield, which is because the particles deposited on the wall of the spraying tower were collected separately and finally not considered due to its low oxidative quality (results not shown). In the PGSS-drying method, some of the finer particles were blown away by the vented CO_2 and deposited in the condenser. This wet powder was not collected, slightly reducing the final yield. In the case of the freeze-dried particles, the observed yield is very close to unity. This trend was also observed by other authors (Lévai et al., 2017) and may be attributed to the one-pot processing and the preservation of the emulsion structure during freezing.

Regarding the bioactive loading, it is close to the maximum theoretical loading of 200 mg/g sample in all cases, and no statistical differences ($p < 0.05$) are observed no matter the drying method used to obtain the particles. Nevertheless, the spray-dried

502 particles present a slightly lower average value, which may be attributed to the higher
503 moisture content that will be discussed next. On the other hand, the freeze-dried
504 particles present the highest fish oil concentrate loading, which is possibly linked to the
505 aforementioned preservation of the emulsion integrity.
506

507 ***3.3.2. Moisture content***

508 The moisture content of the particles prepared with different drying methods is showed
509 in Table 1. The spray-dried particles showed the highest residual humidity, whereas the
510 PGSS-drying technique gave the lowest moisture value. Humidity values for the spray-
511 dried particles found in this work are higher than those reported in the literature, which
512 are usually around 1-3 % (Carneiro et al., 2013; Hogan, McNamee, O'Riordan, &
513 O'Sullivan, 2001). In the case of the freeze-dried particles, no significant difference in
514 the final humidity was found ($p < 0.05$), no matter the freezing method used
515 (conventional at -20 ºC or with liquid nitrogen).
516

517 ***3.3.3. Encapsulation efficiency***

518 Encapsulation efficiency is one of the most important quality parameters in
519 encapsulated fish oil and *n*–3 PUFA concentrates. The presence of free oil may
520 adversely affect the physical properties of the final product, such as flowability and bulk
521 density, and would also enhance lipid oxidation (Y. Wang et al., 2016). Table 1 shows
522 the initial encapsulation efficiency of the drying methods proposed in this work.

523 In general, high initial encapsulation efficiencies, no matter the drying method used,
524 were obtained. It can be noticed that the powder obtained by freeze-drying with
525 conventional -20ºC freezing presents a significantly lower ($p < 0.05$) initial

encapsulation efficiency, with EE = 95.8 ± 0.2 % (Table 1). As it has been previously mentioned, it is likely that partial destabilization of the emulsion and release of small amounts of *n*–3 PUFA concentrate may have happened, probably due to the mechanical and hygroscopic forces caused by the growing of large water crystals during the slow freezing process. By comparison, freeze-dried particles obtained with liquid nitrogen present the highest encapsulation efficiency with 98.6 ± 0.1 % (Table 1), which reflects that the emulsion casting is preserved with a rapid and deep freezing step. Similar results have been also obtained by Lévai *et al.* (Lévai et al., 2017) dealing with freeze-dried quercetin encapsulated in soybean lecithin. Still, more than 95 % of the total *n*–3 PUFA concentrate loading was encapsulated by conventional freeze-drying, and almost 98 % encapsulation efficiency was obtained by PGSS-drying (97.9 ± 0.3 %), which is similar to the EE value of the spray-dried microparticles (97.5 ± 0.1 %). Carneiro *et al.* (Carneiro et al., 2013) compared combinations of maltodextrin and Hi-Cap and other wall materials to encapsulate flaxseed oil by spray-drying, finding Hi-Cap as the best in terms of EE, with 95.7 %. Results obtained in this work are slightly higher in all cases except for conventionally freeze-dried particles, which may be attributed to the optimized US-assisted emulsification process.

Surface oil of the dried particles has been analyzed over time during 28 days of storage at 4ºC in darkness and ambient oxygen concentration to check if some of the *n*–3 PUFA concentrate could have been released. Results obtained are summarized in Fig. S-2 of the supplementary material. As Fig. S-2 shows, spray-dried particles released around 2% of the total encapsulated *n*–3 PUFA concentrate during the first 7 days and then the release continued at a lower rate, down to 94 % encapsulated oil after 28 days. In the case of the conventionally freeze-dried particles, a slight decrease in the encapsulated oil can be seen after the second week of storage; whereas for the PGSS- and freeze-

551 dried particles frozen with liquid N_2, no significant changes in the encapsulation
552 efficiency were noted during the first 21 days and only a slight decrease started to occur
553 after the fourth week of storage.

554

555 ***3.3.4. Particle Size Analysis***

556 The particle size distribution plot of PGSS-dried and spray dried particles is provided in
557 Fig. 2. Particle mean diameters ($d_{0.5}$) varied from 28.605 μm for PGSS-dried particles to
558 35.375 μm for the spray-dried particles. The span value of the PGSS-dried particles
559 (1.663) was also lower than that of the spray-dried particles (6.082).

560 The microparticles produced by spray drying showed a bimodal distribution with a
561 group of particles centered around 30 μm and a second population around 250 μm. This
562 justifies the high span value and may be linked to particle swelling during drying as
563 well as to agglomeration due to the higher moisture content. This agglomerated clusters
564 are also visible in the SEM images showed in Fig. 3b and discussed in the next section.

565 On the other hand, the PGSS-dried particles show a monomodal particle size
566 distribution with smaller mean diameter. As it has been reported in previous works (de
567 Paz et al., 2012), the effective atomization caused by CO_2 vaporization may have led to
568 the production of smaller and monodisperse particles.

569

570 ***3.3.5. Particle morphology (SEM)***

571 Visual morphology of the dried powders can be observed in the SEM micrographs
572 (Fig. 3). Both PGSS- and spray-dried particles present spherical morphology. For the
573 PGSS-dried particles, small spheres with diameters ranging from 2 μm to 5 μm can be

observed together with some larger agglomerates around 10-20 μm diameter (Fig. 3a). Fractured particles are also seen in some micrographs, showing a porous internal structure in which the *n*–3 PUFA concentrate is probably encapsulated. As it has been also observed in the particle size analysis, spray-dried particles show more variance in size. A small population of microparticles around 2 μm was detected together with some specimens larger than 20 μm and particle clusters around 150 μm (Fig. 3b), which is also in accordance with the results obtained in the particle size analysis (section 3.3.4). This variety in size has been also reported in the literature (Carneiro et al., 2013), and seems to be a typical characteristic of particles produced by spray drying. Spray-dried particles also showed a rougher surface than PGSS-dried samples, with more imperfections or 'teeth'. These surface depressions are associated to the collapse of the particle hollow core once the crust is formed during the initial stages of drying. Similar morphological characteristics have been also found in the literature, either with OSA-starch as encapsulating agent (Carneiro et al., 2013), or with other materialas such as β-glucans (Salgado, Rodríguez-Rojo, Alves-Santos & Cocero, 2015).

In the case of the freeze-dried particles, larger and more irregular particles have been produced. Conventionally freeze-dried powder presents a flakey or scaly appearance, forming planar structures with some dimensions being larger than 100 μm (Fig. 3c). Some dents can be seen in the surface of several particles, probably corresponding to the voids left by water crystals after sublimation. In larger magnifications (3000x) a porous internal structure can be also appreciated, being the *n*–3 PUFA concentrate likely encapsulated inside these vesicles. In the case of the freeze-dried powder frozen with liquid N_2 (Fig. 3d), a powder finer than the conventionally frozen (Fig. 3c) has been obtained. Some particles show an alveolar structure, which may have been formed

by liquid nitrogen boiling during freezing of the O/W emulsion. These alveolar holes present diameters around 5-7.5 µm.

3.3.6. Differential Scanning Calorimetry (DSC)

DSC runs of PGSS-dried particles, modified OSA-starch (Hi-Cap 100) used as a carrier, and *n*–3 PUFA concentrate revealed cold-crystallization, glass-transition (gelatinization) and melting peaks. The peak temperatures of these thermal events are summarized in Table 2. Endothermic peaks near 80 ºC were observed in the PGSS-dried and Hi-Cap 100 samples, which probably correspond to the glass transition (gelatinization) of OSA-starch. A second endothermic peak was found around 220 ºC in both PGSS-dried particles and Hi-Cap 100, which may be linked to the melting of OSA-starch. Similar glass-transition and melting temperatures have been reported in the literature for this polymer (Yu & Christie, 2001).

In the lower temperature range, an exothermic cold-crystallization peak was noticeable for the *n*–3 PUFA concentrate and for the PGSS-dried particles, which may correspond to some lipid compound of the *n*–3 PUFA concentrate transitioning from liquid to solid state. This assumption can be corroborated by the studies of Tolstorebrov *et al.* (Tolstorebrov, Eikevik, & Bantle, 2014), in which cold-crystallization peaks in the range -75 to -55 ºC have been reported for some olein-, linolenin-, and linolein-containing tryacylglycerides, which are minoritary constituents of the *n*–3 PUFA concentrate (Table S-1a). The slightly lower crystallization temperature observed in the PGSS-dried particles compared to the *n*–3 PUFA concentrate alone (Algatrium™ Plus) is probably linked to the particle shell offering heat transfer resistance to the encapsulated oil, and thus delaying the cold crystallization event.

622

623 **3.4. Oxidative stability of the dried powders**

624 Peroxide value (PV) and thiobarbituric acid reactive substances (TBARS) have been
625 systematically determined in the PGSS-dried powders with and without ascorbic acid
626 (AA) during 28 days of storage at 4 ºC and dark conditions. In order to determine the
627 initial oxidative status, PV and TBARS were measured in the *n*–3 PUFA concentrate
628 and in the original emulsion right after US-assisted emulsification. With the purpose of
629 comparing the different drying methods used in this work, PV and TBARS of the spray-
630 dried and the freeze-dried particles were measured after formulation of the powders
631 (day 0) and after 28 days of storage under the same conditions as the PGSS-dried
632 particles (4ºC, darkness). Results obtained are summarized in Fig. 4.

633 Fig. 4a shows that PV increases from 1.64 ± 0.05 meq O_2/kg oil in the *n*–3 PUFA
634 concentrate up to 5.6 ± 0.3 meq O_2/kg oil during the US-assisted emulsification process,
635 which slightly surpasses the maximum limit of 5 meq O_2/kg oil for fish oil concentrates
636 intended for direct human consumption (*Codex Alimentarius Comission*, 2017). It is
637 likely that the high energy input involved in the ultrasonication process promoted a
638 temperature increase that may negatively affect the oxidative status of the *n*–3 PUFA
639 concentrate (Abbas et al., 2013). As a strategy to prevent primary oxidation during US-
640 assisted emulsification, 20 mM ascorbic acid (AA) was added to the emulsion
641 formulation. AA concentration was selected based on Uluata *et al.* (Uluata et al., 2015)
642 studies on lipid oxidation in O/W emulsions.
643 As it can be seen in Fig. 4a inset (O/W emulsion), the antioxidant successfully protected
644 the *n*–3 PUFA concentrate and even reduced the PV of the emulsion down to 0.19 ±
645 0.03 meq O_2/kg oil. This behaviour has been also observed by Uluata *et al.* in O/W
646 emulsions with AA (Uluata et al., 2015) and it is likely related to AA's ability to

647 inactivate free radicals such as lipid hydroperoxides. Other mechanisms can be also
648 involved in the observed antioxidant activity, since AA can act as an oxygen scavenger
649 thanks to the enediol group in carbons 2 and 3 (Johnson, 1995; Liao & Seib, 1988), or
650 even play a synergistic role by means of regenerating other antioxidants such as the
651 tocopherol originally present in the *n*–3 PUFA concentrate (Reische, Lillard, &
652 Eitenmiller, 2008). However, it is not easy to determine which of these pathways is
653 taking place in any given food system (Uluata et al., 2015) and it is likely that all of
654 them occur simultaneously.

655 If we focus on the PV results obtained after formulation of the dried particles (Fig. 4a
656 day 0), it can be seen that PGSS-drying promoted a slight PV increase up to 5.9 ± 1.5
657 meq O_2/kg oil in the emulsion without AA, although this value is not significantly
658 different ($p < 0.05$) from the PV of the original emulsion. Furthermore, AA addition had
659 a significant ($p < 0.05$) effect on the PV of the PGSS-dried particles, since only a slight
660 increase from 0.19 ± 0.03 to 0.5 ± 0.1 meq O_2/kg oil was observed in the PGSS-dried
661 particles with antioxidant (Fig. 4a day 0). On the other hand, the spray-drying process
662 yielded particles with much lower oxidative quality (PV = 28.0 ±1.6 meq O_2/kg oil). As
663 some authors have pointed out for the spray-drying process (Drusch & Berg, 2008; H.
664 Wang et al., 2011), it is likely that the rapid formation of the particle shell increased the
665 resistance to evaporation of water trapped inside the particle core, promoting a rapid
666 temperature increase in the particles and prolonging the *n*–3 PUFA exposure to high
667 temperatures, thus promoting oxidation and increasing the PV after spray-drying
668 formulation. The freeze-drying process with liquid nitrogen achieved good results, with
669 PV = 4.6 ± 1.8 meq O_2/kg oil, which is not statistically different ($p < 0.05$) from that of
670 the original emulsion (Fig. 4a day 0). This result can be related to the freeze-drying
671 process being a degradation-free technology, since the samples are not submitted to

high processing temperatures and processed in absence of light and in an almost inert atmosphere due to vacuum conditions. Unexpectedly, the conventionally frozen emulsion did overcome oxidation despite the favourable processing conditions, showing a PV = 12.4 ± 1.5 meq O_2/kg oil (Fig. 4a day 0). This is likely due to oxygen contact during the conventional freezing step, in which the samples were held overnight at -20ºC under ambient oxygen concentration.

In view of the results (Fig. 4a day 0), we can infer that PGSS-drying is a suitable method to formulate dried particles loaded with *n*–3 PUFAs, more so if we combine the mild processing conditions with the addition of an antioxidant such as AA. As it has been previously stated, the short residence time of the O/W emulsion in the PGSS-drying system as well as the inert CO_2 atmosphere prevent the loaded bioactive compounds from degradation (Weidner, 2009) and as such, the *n*–3 PUFA concentrate can be successfully protected from oxidation.

Oxidative stability of the PGSS-dried particles was monitored during 28 days of storage in darkness at 4 ºC (Fig. 4a days 1-28). Results obtained showed a sustained increase of primary oxidation, reaching values of PV = 25.2 ± 0.7 meq O_2/kg oil after 28 days of storage (Fig. 4a). On the other hand, AA successfully protected the PGSS-dried particles from primary oxidation during storage, being the values found significantly lower ($p < 0.05$) than those of the PGSS-dried particles without antioxidant. The highest PV was found after 14 days of storage and was 2.5 ± 0.5 meq O_2/kg oil, still below the maximum allowable limit according to legislation, and remained with no significant changes ($p < 0.05$) during the rest of the 28-day storage period, reaching a final value of 2.2 ± 0.3 meq O_2/kg oil (Fig. 4a).

695 Comparing the primary oxidation of the particles obtained by the different drying
696 methods after 28 days of storage, we can see the same trend as in the PV analysis after
697 formulation, although PV increased in all samples (Fig. 4a days 1-28). Freeze-dried
698 particles frozen with liquid nitrogen maintained a relatively low PV of 16.9 ± 0.8 meq
699 O_2/kg oil, which is likely linked to the good encapsulation efficiency and the
700 preservation of the physical structure of the emulsion thanks to the fast and deep-
701 cooling effect of liquid nitrogen. The same was not true for the conventionally freeze-
702 dried particles, with PV = 37.7 ± 3.7 meq O_2/kg oil after 28 days of storage. Spray-dried
703 particles showed the highest PV with 66.0 ± 0.4 meq O_2/kg oil after 28 days of storage.
704 The higher oxidation rates of these two samples (spray-drying and conventional freeze-
705 drying) are probably due to the high starting PV (day 0) as well as their lower
706 encapsulation efficiency, which implies more oil in the particle surface susceptible to
707 oxidation. A similar encapsulation efficiency vs. oxidation rate inverse relationship has
708 been observed by other authors (Yang & Ciftci, 2017). However, PGSS-dried and
709 freeze-dried particles with liquid nitrogen exhibited high encapsulation efficiencies (up
710 to 98%), and still encapsulated *n*–3 PUFA concentrate was not fully protected against
711 primary oxidation (PV after 28 days = 25.2 ± 2.2 and 16.9 ± 0.8 meq O_2/kg oil,
712 respectively). This trend can be explained by taking into account not only the oxidation
713 of the oil present in the particle surface, but also oxygen diffusion through the
714 encapsulating material. It must be also pointed out that the fish oil concentrate used in
715 this work is extremely rich in *n*–3 PUFAs, which are highly prone to oxidation. This
716 highly sensitive-to-oxidation fatty acid profile may also offer an explanation to the
717 higher oxidation rates obtained in this work compared to other studies, even with no
718 accelerated storage (Carneiro et al., 2013; Yang & Ciftci, 2017).

719 TBARS analysis results are summarized in Fig. 4b. Although there is no legal
720 maximum limit for this parameter in food products, we can take the values of 10 µmol
721 MDA equiv/kg fish and 1-2 µmol MDA equiv/g fat given in the FAO guidelines (Huss,
722 1995) as an orientative basis to evaluate rancidity of the *n*–3 PUFA concentrate (1 µmol
723 MDA equiv/g fat corresponds to 72.06 mg MDA/kg oil). From Fig. 4b we can see that
724 initial TBARS of the *n*–3 PUFA concentrate lay below this rancidity limit (TBARS =
725 41.1 ± 2.7 mg MDA/kg oil). US-assisted emulsification slightly increased the TBARS
726 value up to 54.8 ± 0.6 mg MDA/kg oil in the formulation without AA, whereas the
727 addition of AA yielded particles with TBARS = 42.8 ± 1 mg MDA/kg oil (Fig. 4b day
728 0). In view of the results, AA addition slowed down secondary oxidation during the
729 ultrasonication step since no significant difference (p <0.05) between the AA-added
730 emulsion and the *n*–3 PUFA concentrate was found (Fig. 3b inset).

731 Among the dried powders (Fig. 4b, day 0), spray-dried particles showed the highest
732 secondary oxidative status with a TBARS value of 88.5 ± 6.0 mg MDA/kg oil, which is
733 above the FAO rancidity limit (Huss, 1995). PGSS-drying process slightly increased
734 TBARS up to 59.4 ± 4.4 mg MDA/kg oil, whereas the addition of AA did not make any
735 statistically significant difference (p < 0.05). Both PGSS-drying with and without AA,
736 and freeze-dried powder with liquid N_2 showed no statistically significant differences
737 with the original emulsion, which gives an idea of the protective effect of these drying
738 techniques against secondary oxidation. On the contrary, the conventionally frozen
739 particles were not successfully protected, and TBARS increased up to 74.5 ± 3.5 mg
740 MDA/kg oil after the conventional freeze-drying process.

741 Secondary oxidation products were also monitored in the PGSS-dried particles during
742 the 28-day storage period. In Fig. 4b (days 1-28), we can see that TBARS in the PGSS-
743 dried particles without AA did not significantly increase (p < 0.05) up to the second

744 week of storage, when TBARS value raised from 69.2 ± 1.4 up to 110.9 ± 1.8 mg
745 MDA/kg oil, reaching a final value of 141.0 ± 1.9 mg MDA/kg oil after 28 days of
746 storage. On the other hand, AA addition delayed secondary oxidation for the first 14
747 days of storage, obtaining significantly lower ($p < 0.05$) TBARS values than those of
748 the control sample without antioxidant, yet increasing thereafter and even exceeding the
749 control after 28 days of storage (TBARS = 141.0 ±1.9 mg MDA/kg oil). As previously
750 mentioned, this behavior has been observed by other authors when studying the effect
751 of ascorbic acid on lipid oxidation in O/W emulsions, especially in presence of
752 transition metals such as iron and copper (Mei et al., 1998; Uluata et al., 2015). Uluata
753 *et al.* (Uluata et al., 2015) provide an explanation related to the ability of AA to reduce
754 metal ions, making them more reactive towards peroxides and hydroperoxides.
755 According to this proposed mechanism, reduced metallic species would decompose
756 peroxides and hydroperoxides into secondary oxidation products, increasing the
757 observed TBARS and preventing the accumulation of primary oxidation intermediaries
758 (Uluata et al., 2015). This behavior has been also observed in this work, although no
759 metals were added to the O/W emulsion. However, and according to inductively
760 coupled plasma mass spectrometry (ICP-MS) analysis (Table S-2), metal traces are
761 present in the encapsulating material, enabling this hypothesis.

762 Additionally, it has been found that spray-dried and conventionally freeze-dried
763 particles underwent secondary oxidation during the 28-day storage period, with final
764 TBARS values of 137.2 ± 4.7 mg MDA/kg oil and 166.6 ± 0.3 mg MDA/kg oil,
765 respectively (Fig. 4b days 1-28). Again, this high secondary oxidation status might be
766 linked to the poorer encapsulation efficiency of those methods. On the other hand,
767 freeze-dried particles frozen with liquid N_2 showed good stability against secondary

768 oxidation during storage, maintaining a TBARS value of 79.6 ± 2.4 during 28 days of
769 storage at 4ºC.

770

771 **4. Conclusion**

772 Particles from Gas-Saturated Solutions (PGSS)-drying has been used to encapsulate
773 omega–3 polyunsaturated fatty acids (*n*–3 PUFAs) into octenyl-succinic-anhydride
774 (OSA) starch, obtaining a solid powder with high bioactive load.

775 Similar encapsulation efficiencies (EE) and spherical morphologies have been obtained
776 by PGSS and spray-drying.

777 Freeze-dried particles showed irregular morphology. Slow conventional freezing
778 destabilizes the O/W emulsion and negatively affects EE. DSC analysis of the PGSS-
779 dried particles successfully identified cold crystallization of the *n*–3 PUFA concentrate
780 as well as gelatinization and melting peaks of OSA-starch.

781 PGSS-drying method offers low drying temperature and an intrinsically inert
782 atmosphere, which avoid oxidative degradation of *n*–3 PUFAs during processing, as
783 demonstrated by the oxidative stability analyses. Conventional freeze-drying method
784 yielded particles with low oxidative stability, whereas freezing with liquid N_2 resulted
785 in a powder with oxidative stability comparable to PGSS-dried particles. Combined
786 with the addition of natural antioxidants such as ascorbic acid, the PGSS-drying
787 technique rises as a suitable method to formulate *n*–3 PUFAs in solid form and protect
788 them against oxidation during shelf life.

789

Acknowledgements

To Junta de Castilla y León and the European Regional Development Fund for financial support of the project BU055U16 and ÓB's post-doctoral contract. To Spanish Ministry of Economy and Competitiveness for RM's pre-doctoral contract [BES-2013-063937] and EP's post-doctoral contract [FJCI-2014-19850].

References

Abbas, S., Hayat, K., Karangwa, E., Bashari, M. & Zhang, X. (2013). An overview of ultrasound-assisted food-grade nanoemulsions. *Food Engineering Reviews*, *5*, 139–157. https://doi.org/10.1007/s12393-013-9066-3

AOAC International. (2005). *Official methods of analysis of the Association of Official Analytical Chemists. AOAC Official Method 925.32. Fat in eggs, acid hydrolysis method* (Vol. 6). Washington, DC.

AOAC International. (2012). *Official methods of analysis of the Association of Official Analytical Chemists. AOAC Official Method 2012.13. Determination of labeled fatty acids content in milk products and infant formula*. Washington, DC.

Baik, M. Y., Suhendro, E. L., Nawar, W. W., McClements, D. J., Decker, E. A., & Chinachoti, P. (2004). Effects of Antioxidants and Humidity on the Oxidative Stability of Microencapsulated Fish Oil. *JAOCS, Journal of the American Oil Chemists' Society*, *81*(4), 355–360. https://doi.org/10.1007/s11746-004-0906-7

Bakry, A. M., Abbas, S., Ali, B., Majeed, H., Abouelwafa, M. Y., Mousa, A., & Liang, L. (2016). Microencapsulation of Oils: A Comprehensive Review of Benefits, Techniques, and Applications. *Comprehensive Reviews in Food Science and Food Safety*, *15*(1), 143–182. https://doi.org/10.1111/1541-4337.12179

Carneiro, H. C. F., Tonon, R. V, Grosso, C. R. F., & Hubinger, M. D. (2013). Encapsulation efficiency and oxidative stability of flaxseed oil microencapsulated by spray drying using different combinations of wall materials. *Journal of Food Engineering*, *115*(4), 443–451. https://doi.org/10.1016/j.jfoodeng.2012.03.033

Chatterjee, S., & Judeh, Z. M. A. (2015). Encapsulation of fish oil with N -stearoyl O-butylglyceryl chitosan using membrane and ultrasonic emulsification processes. *Carbohydrate Polymers*, *123*, 432–442. https://doi.org/10.1016/j.carbpol.2015.01.072

Codex Alimentarius Comission, *Standard for fish oils Codex Stan 329-2017*. (2017). Rome, Italy.

de Paz, E., Martín, Á., & Cocero, M. J. (2012). Formulation of β-carotene with soybean lecithin by PGSS (Particles from Gas Saturated Solutions)-drying. *The Journal of Supercritical Fluids*, *72*, 125–133. https://doi.org/10.1016/j.supflu.2012.08.007

de Paz, E., Martín, T., Bartolomé, A., Largo, M., & Cocero, M. J. (2014). Development of water-soluble β-carotene formulations by high-temperature, high-pressure

emulsification and antisolvent precipitation. *Food Hydrocolloids*, *37*, 14–24. https://doi.org/10.1016/j.foodhyd.2013.10.011

Drusch, S., & Berg, S. (2008). Extractable oil in microcapsules prepared by spray-drying: localisation, determination and impact on oxidative stability. *Food Chemistry*, *109*, 17–24. https://doi.org/10.1016/j.foodchem.2007.12.016

Drusch, S., Serfert, Y., Scampicchio, M., Schmidt-Hansberg, B., & Schwarz, K. (2007). Impact of physicochemical characteristics on the oxidative stability of fish oil microencapsulated by spray-drying. *Journal of Agricultural and Food Chemistry*, *55*, 11044–11051.

EFSA Panel on Dietetic Products Nutrition and Allergies (NDA), Scientific Opinion on the substantiation of health claims related to eicosapentaenoic acid (EPA), docosahexaenoic acid (DHA), docosapentaenoic acid (DPA) etc. (2010). *EFSA Journal*, *8*(10), 1796. https://doi.org/10.2903/j.efsa.2010.1796

Encina, C., Vergara, C., Giménez, B., Oyarzún-Ampuero, F., & Robert, P. (2016). Conventional spray-drying and future trends for the microencapsulation of fish oil. *Trends in Food Science & Technology*, *56*, 46–60. https://doi.org/https://doi.org/10.1016/j.tifs.2016.07.014

Hogan, S. A., McNamee, B. F., O'Riordan, E. D., & O'Sullivan, M. (2001). Emulsification and microencapsulation properties of sodium caseinate/carbohydrate blends. *International Dairy Journal*, *11*(3), 137–144. https://doi.org/10.1016/S0958-6946(01)00091-7

Huss, H. H. (1995). *Quality and quality changes in fresh fish. FAO Fisheries technical paper - 348, Food and Agriculture Organization of the United Nations*. Rome.

Jafari, S. M., Assadpoor, E., He, Y., & Bhandari, B. (2008). Encapsulation efficiency of food flavours and oils during spray drying. *Drying Technology*, *26*(7), 816–835. https://doi.org/10.1080/07373930802135972

Johnson, L. E. (1995). Food technology of the antioxidant nutrients. *Critical Reviews in Food Science and Nutrition*, *35*(1–2), 149–159. https://doi.org/10.1080/10408399509527694

Ke, P. J., & Woyewoda, A. D. (1979). Microdetermination of thiobarbituric acid values in marine lipids by a direct spectrophotometric method with a monophasic reaction system. *Analytica Chimica Acta*, *106*, 279–284. https://doi.org/10.1016/S0003-2670(01)85011-X

Lévai, G., Martín, Á., Moro, A., Matias, A. A., Gonçalves, V. S. S., Bronze, M. R., … Cocero, M. J. (2017). Production of encapsulated quercetin particles using supercritical fluid technologies. *Powder Technology*, *317*, 142–153. https://doi.org/10.1016/j.powtec.2017.04.041

Liao, M.-L., & Seib, P. A. (1988). Chemistry of L-ascorbic acid related to foods. *Food Chemistry*, *30*(4), 289–312. https://doi.org/10.1016/0308-8146(88)90115-X

Löliger, J., & Saucy, F. (1994, April 27). Patent EP0326829B1 Synergetic antioxidant mixture.

Martín, Á., & Weidner, E. (2010). PGSS-drying: Mechanisms and modeling. *The Journal of Supercritical Fluids*, *55*, 271–281. https://doi.org/10.1016/j.supflu.2010.08.008

Mei, L., McClements, D. J., Wu, J., & Decker, E. A. (1998). Iron-catalyzed lipid oxidation in emulsion as affected by surfactant, pH and NaCl. *Food Chemistry*, *61*(3), 307–312. https://doi.org/10.1016/S0308-8146(97)00058-7

Niki, E. (2009). Lipid peroxidation: Physiological levels and dual biological effects. *Free Radical Biology and Medicine*, *47*, 469–484. https://doi.org/10.1016/j.freeradbiomed.2009.05.032

Pocklington, W. D., & Dieffenbacher, A. (1988). Determination of tocopherols and tocotrienols in vegetable oils and fats by high performance liquid chromatography. *Pure and Applied Chemistry*, *60*(6), 877–892. https://doi.org/10.1351/pac198860060877

Rebolleda, S., Rubio, N., Beltrán, S., Sanz, M. T., & González-San José, M. L. (2012). Supercritical fluid extraction of corn germ oil: study of the influence of process parameters on the extraction yield and oil quality. *Journal of Supercritical Fluids*, *72*, 270–277. https://doi.org/10.1016/j.supflu.2012.10.001

Reische, D. W., Lillard, D. A., & Eitenmiller, R. R. (2008). Antioxidants. *Food Lipids*, 413–422. http://doi.org/10.1201/9780203908815.ch15

Rubio-Rodríguez, N., Beltrán, S., Jaime, I., de Diego, S. M., Sanz, M. T., & Carballido, J. R. (2010). Production of omega-3 polyunsaturated fatty acid concentrates: a review. *Innovative Food Science & Emerging Technologies*, *11*(1), 1–12. https://doi.org/10.1016/j.ifset.2009.10.006

Ruxton, C. H. S., Reed, S. C., Simpson, M. J. A., & Millington, K. J. (2004). The health benefits of omega-3 polyunsaturated fatty acids: A review of the evidence. *Journal of Human Nutrition and Dietetics*, *17*(5), 449–459. https://doi.org/10.1111/j.1365-277X.2004.00552.x

Salgado, M., Rodríguez-Rojo, S., Alves-Santos, F. M., & Cocero, M. J. (2015). Encapsulation of resveratrol on lecithin and β-glucans to enhance its action against *Botrytis cinerea*. *Journal of Food Engineering*, 165, 13–21. https://doi.org/10.1016/j.jfoodeng.2015.05.002

Shantha, N. C., & Decker, E. A. (1994). Rapid, sensitive, iron-based spectrophotometric methods for determination of peroxide values of food lipids. *Journal of AOAC International*, *77*, 421–424.

Solaesa, Á. G., Sanz, M. T., Falkeborg, M., Beltrán, S., & Guo, Z. (2016). Production and concentration of monoacylglycerols rich in omega-3 polyunsaturated fatty acids by enzymatic glycerolysis and molecular distillation. *Food Chemistry*, *190*, 960–967. https://doi.org/10.1016/j.foodchem.2015.06.061

Tolstorebrov, I., Eikevik, T. M., & Bantle, M. (2014). A DSC determination of phase transitions and liquid fraction in fish oils and mixtures of triacylglycerides. *Food Research International*, *58*, 132–140. https://doi.org/10.1016/j.foodres.2014.01.064

Türk, M. (2014). *Particle Formation with Supercritical Fluids Challenges and Limitations*. (M. Türk, Ed.), *Supercritical Fluid Science and Technology* (Vol. Volume 6). Elsevier. https://doi.org/https://doi.org/10.1016/B978-0-444-59486-0.00009-7

Uluata, S., McClements, D. J., & Decker, E. A. (2015). How the multiple antioxidant properties of ascorbic acid affect lipid oxidation in oil-in-water emulsions. *Journal*

of Agricultural and Food Chemistry, *63*, 1819–1824. https://doi.org/10.1021/jf5053942

Varona, S., Martín, A., & Cocero, M. J. (2011). Liposomal Incorporation of Lavandin Essential Oil by a Thin-Film Hydration Method and by Particles from Gas-Saturated Solutions. *Industrial & Engineering Chemistry Research*, 50(4), 2088–2097. https://doi.org/10.1021/ie102016r

Wang, H., Liu, F., Yang, L., Zu, Y., Wang, H., Qu, S., & Zhang, Y. (2011). Oxidative stability of fish oil supplemented with carnosic acid compared with synthetic antioxidants during long-term storage. *Food Chemistry*, *128*(1), 93–99. https://doi.org/10.1016/j.foodchem.2011.02.082

Wang, Y., Liu, W., Dong, X., & Selomulya, C. (2016). Micro-encapsulation and stabilization of DHA containing fish oil in protein-based emulsion through mono-disperse droplet spray dryer. *Journal of Food Engineering*, *175*, 74–84. https://doi.org/10.1016/j.jfoodeng.2015.12.007

Weidner, E. (2009). High pressure micronization for food applications. *The Journal of Supercritical Fluids*, *47*, 556–565. https://doi.org/10.1016/j.supflu.2008.11.009

Yang, J., & Ciftci, O. N. (2017). Encapsulation of fish oil into hollow solid lipid micro- and nanoparticles using carbon dioxide. *Food Chemistry*, *231*, 105–113. https://doi.org/10.1016/j.foodchem.2017.03.109

Yu, L., & Christie, G. (2001). Measurement of starch thermal transitions using differential scanning calorimetry. *Carbohydrate Polymers*, *46*, 179–184.

939 Table 1**.** Summary of experimental results.

Emulsion /drying method	**Density (g·cm^{-3})**	**Yield (%)**	**EE (day 0) (%)**	**Bioactive loading (mg/g)**	**Moisture (%)**	**Droplet size analysis**			
						D[4,3]	**D[3,2]**	**$d_{0.5}$ (µm)**	**span**
Original		--		--	--	0.144^{a}	0.114^{a}	0.114^{a}	1.150^{a}
PGSS-drying		61 ± 1	97.9^{b} ± 0.3	191 ± 8	3.3 ± 0.3^{a}	0.227^{b}	0.116^{a}	0.134^{b}	2.197^{d}
Spray-drying	1.091281*	30 ± 1	97.5^{b} ± 0.1	187 ± 3	5.6 ± 0.2^{c}	0.197^{b}	0.112^{a}	0.129^{b}	1.636^{c}
Freeze-drying (-20ºC)		99 ± 1	95.8^{c} ± 0.2	192 ± 2	4.66 ± 0.05^{b}	0.567^{c}	0.121^{b}	0.131^{b}	1.772^{c}
Freeze-drying) (liq N_2)		99 ± 1	98.6^{a} ± 0.1	192 ± 2	4.7 ± 0.1^{b}	0.146^{a}	0.107^{a}	0.118^{a}	1.291^{b}

* Standard uncertainty is $u(\rho) = \pm 0.000002$ g·cm^{-3}

^{a,b,c,d} Different upper-scripts in the same column denote statistically significant differences at $p < 0.05$

940

941

942

943 **Table 2.** Peak temperatures of the thermal events observed in the PGSS-dried powder loaded with *n*–3
944 PUFA concentrate (PGSS-drying), the carrier alone (Hi-Cap™ 100), and the *n*–3 PUFA concentrate alone
945 (Algatrium™ Plus).

	Peak temperature (°C)		
Sample	**Cold crystallization**	**Glass transition**	**Melting**
PGSS-dried particles	-72.99	76.57	223.55
Hi-Cap™ 100	n.d.	78.83	217.05
Algatrium™ Plus	-71.42	n.d.	n.d.

n.d.: not detected

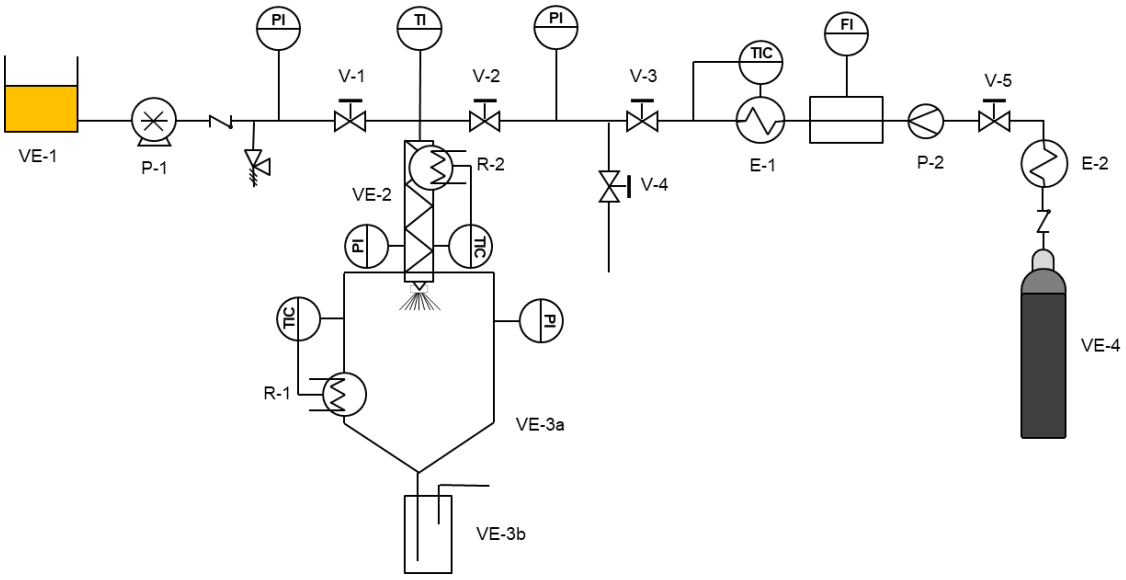

Figure 1. Schematic diagram of the PGSS-drying apparatus. VE-1: O/W emulsion vessel, VE-2: static mixer, VE-3: a) spraying tower, b) condenser, VE-4: CO_2 vessel, P-1: O/W emulsion pump, P-2: CO_2 pump, V-: process valve, E-: heat exchanger, R-: electrical resistance, PI: pressure indicator, TI(C): temperature indicator (and controller).

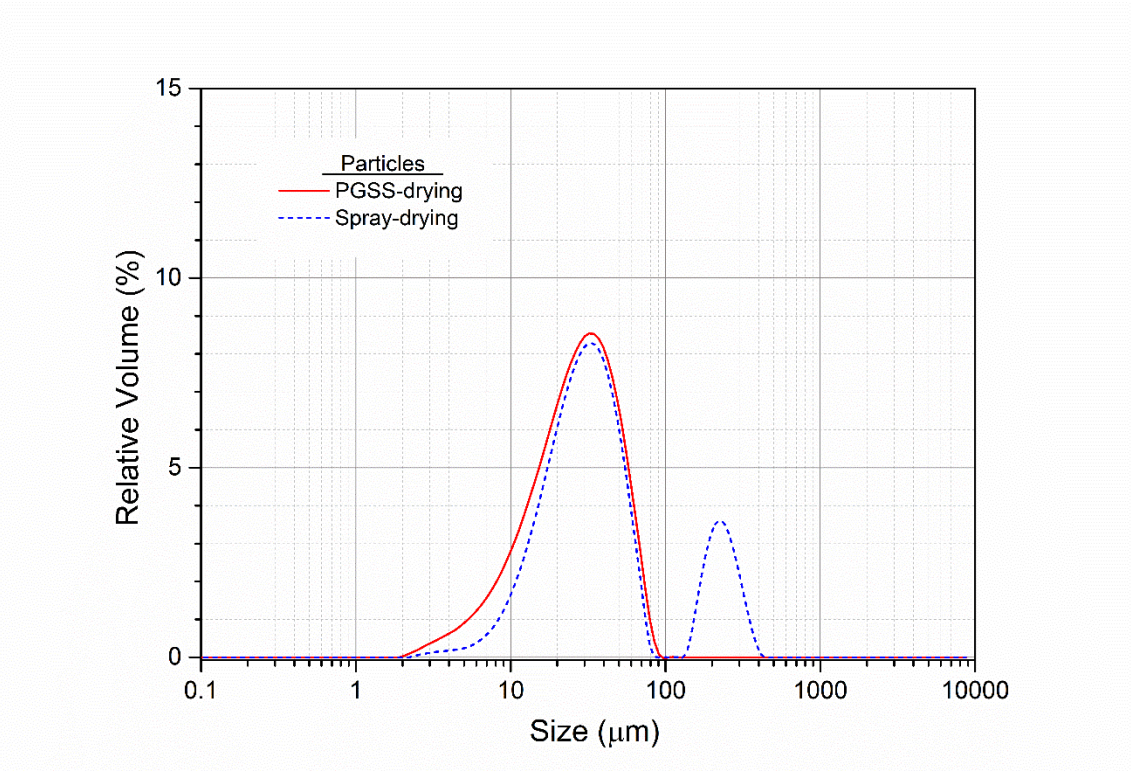

Figure 2. Particle size distribution plot of the particles obtained by PGSS-drying and by spray-drying.

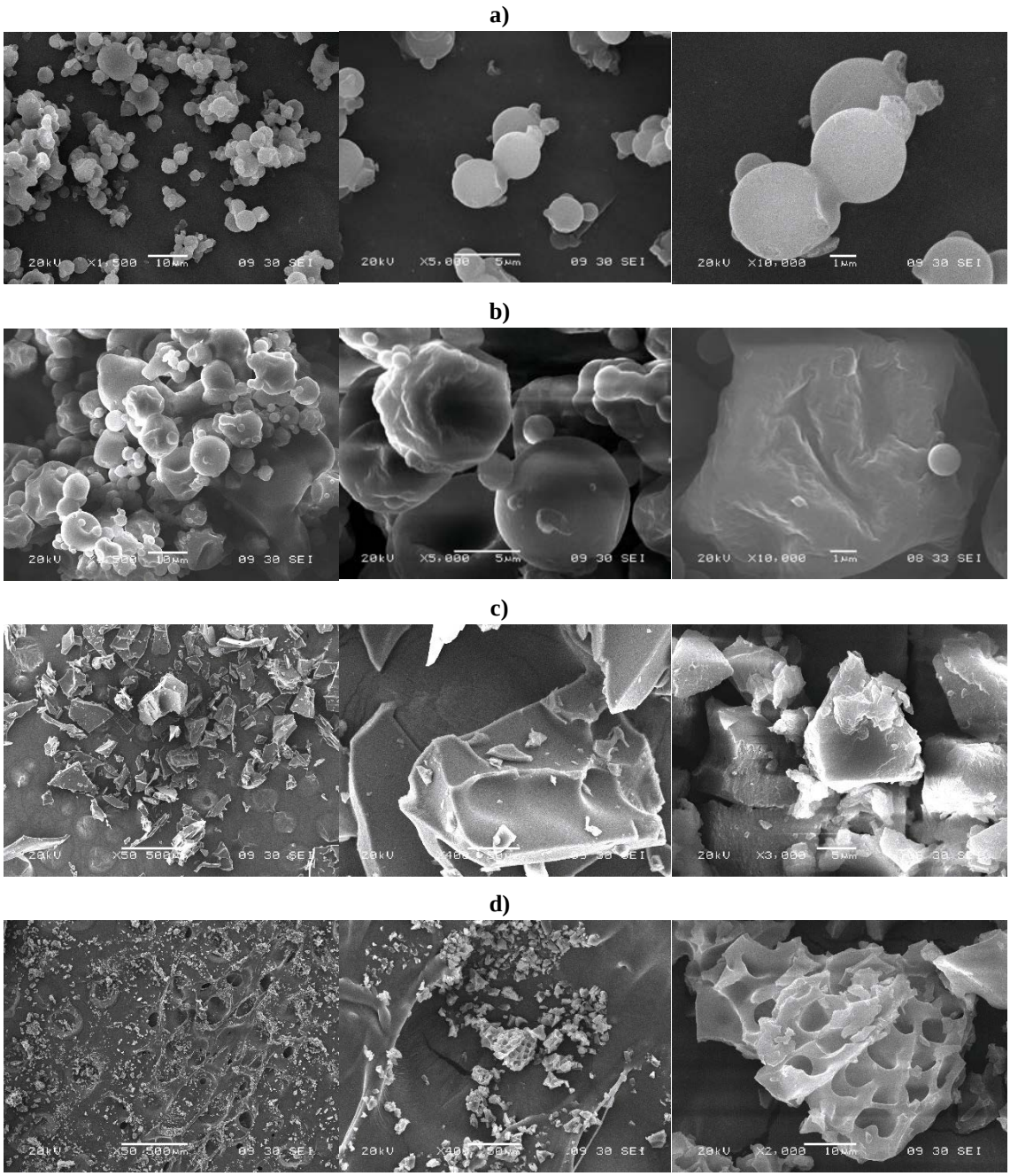

Figure 3. SEM micrographs of the dried powders. **a)** powder obtained by PGSS-drying, **b)** powder obtained by spray-drying; from left to right, 1500, 5000 and 10000x magnifications. **c)** powder obtained by conventional freeze-drying (50, 400 and 3000x). **d)** powder obtained by freeze-drying with liquid N_2; (50, 400 and 2000x).

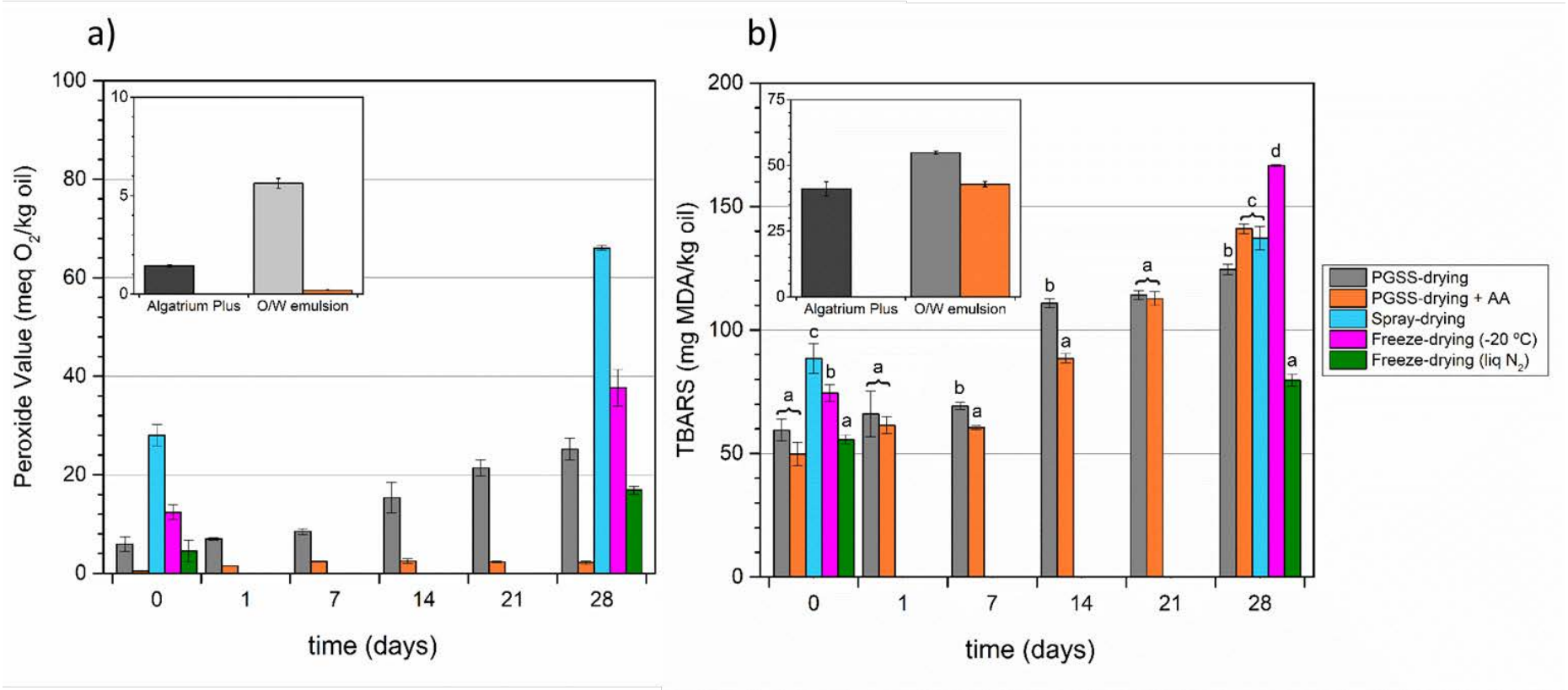

Figure 4. a) Peroxide Value (PV) and **b)** Thiobarbituric acid reactive substances (TBARS) content of the powders obtained by the different drying methods right after drying (day 0) and during storage at 4ºC in darkness and ambient oxygen conditions (days 1-28). Samples were reconstituted the day of analysis keeping the water:carrier:*n*–3 PUFA concentrate proportion the same as the original (70:24:6 wt.). Different letters denote statistically significant differences at $p < 0.05$. **Insets:** PV and TBARS of the *n*–3 PUFA concentrate (Algatrium™ Plus), and the original US-assisted O/W emulsions without and with ascorbic acid (AA).